Journal of Molecular Structure, 176 (1988) 159–179
Elsevier Science Publishers B.V., Amsterdam — Printed in The Netherlands

VIBRATIONAL SPECTRA, MOLECULAR STRUCTURE AND CONFORMATION OF GASEOUS 3-THIOCYANATOPROPYNE (PROPARGYLTHIOCYANATE)

T. MIDTGAARD, G. GUNDERSEN and C. J. NIELSEN

Department of Chemistry, University of Oslo, P.O. Box 1033 Blindern, 0315 Oslo 3 (Norway)

(Received 14 September 1987)

ABSTRACT

3-Thiocyanatopropyne has been prepared and the IR and Raman spectra recorded in the region 4000–40 cm^{-1} and interpreted in terms of two conformers, *anti* and *gauche*, present in the vapour and in the liquid.

Electron diffraction shows that the title compound exists as a mixture of two conformers in the vapour phase: 55(6)% *gauche* with a dihedral angle $\theta_{CCSC}=53(5)^\circ$ and 45(6)% *anti* with $\theta_{CCSC}=180^\circ$ (fixed) at 303 K. Neglecting conformational entropy differences other than the statistical weight of two for *gauche*, this corresponds to an energy difference of 1.24 kJ mol^{-1}, *anti* being marginally the low-energy form. The structural parameters for the two conformers are assumed to differ only by their torsion angle values, and some of the more important bond distances and angles are (r_a and $\angle_\alpha$): $l_{C\equiv N}=116.8(4)$, $r_{C\equiv C}=120.7(5)$, $r_{C-C}=144.4(4)$, $r_{C(sp)-S}=168.9(3)$ and $r_{C(sp^3)-S}=183.6(3)$ pm; and $\angle$C–C–S=112.7(6)° and $\angle$C–S–C=97.4(10)°. The r.m.s. torsional angle amplitudes are $\delta_{gauche}=13(4)^\circ$ and $\delta_{anti}=20(7)^\circ$.

INTRODUCTION

Literature data on the vibrational spectra, structure and conformation of organic thiocyanates are surprisingly scant. Thorough interpretations of the vibrational spectra have been carried out for methyl- [1–5], ethyl- [5–9], isopropyl- [9] and benzylthiocyanate [10]. The vapour phase structure of methylthiocyanate has been determined by microwave spectroscopy [11] and, to our knowledge, only six molecules containing the CH_2–SCN fragment are found in the Cambridge file on crystal structure data [12–17].

Organic thiocyanates also present a conformational problem with conformational possibilities around the C–S(CN) bond. Ethylthiocyanate, which has been a matter of controversy over the past two decades [6–9, 18], exists as a mixture of *gauche* and *anti; gauche* being the more stable by 4.2 kJ mol^{-1} in the vapour [6,19] and by 7.0 kJ mol^{-1} in the liquid [7]. Isopropylthiocyanate has likewise been shown to exist in two conformations in the liquid with an enthalpy difference of 5.7 kJ mol^{-1} [9]. However, it is not known for cer-

0022-2860/88/$03.50

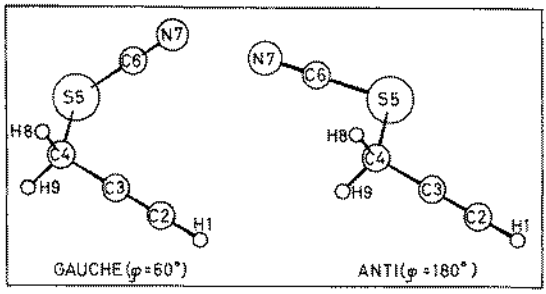

Fig. 1. Views of the *gauche* and *anti* forms of 3-thiocyanatopropyne (TCP) with the numbering of the atoms as used in the interatomic distance specifications.

tain which conformer is the more stable. NMR studies on 2-phenylethylthiocyanate [20] and on the 1,2-dithiocyanato-1-phenylpropanes [21] reveal the solvent to be the determining factor with regard to the preferred conformation in solution.

In the present study of 3-thiocyanatopropyne (TCP), which can exist in *gauche* and *anti* forms as shown in Fig. 1, we have employed the complementary methods of vibrational spectroscopy and gas-phase electron diffraction (GED). The latter method gives direct information about the conformational composition of the gas and the geometry of the molecules. Analysis of the vibrational spectroscopic data also yields information about the conformational equilibria and in addition vibrational amplitude parameters and other quantities required to carry out shrinkage corrections so that an altogether more reliable structure determination by GED can be achieved.

EXPERIMENTAL

Preparative details

Caution: 3-Thiocyanatopropyne permeates many plastics and has a very obnoxious odor that clings to the skin and may ruin the social life for days.

TCP was synthesized from 3-bromopropyne and potassium thiocyanate in an aqueous solution as previously described [22]. After distillation (b.p. = 68 °C/9 mm Hg) the purity, checked by GC, was better than 99%. The deuterated compound, 3-thiocyanatopropyne-1[^{2}H] (TCPD), was synthesized in an analogous manner from 3-bromopropyne-1-[^{2}H], which in turn was prepared via the lithium salt and D_2O.

The compound polymerized/decomposed upon heating and it was not possible to obtain even traces of the isothiocyanate by a thermal rearrangement.

Spectra

Infrared spectra of TCP were recorded on a Perkin-Elmer model 225 spectrometer (5000–200 cm^{-1}) and with a Bruker IFS 114C interferometer (600–20 cm^{-1}). Spectra were obtained of the liquid using sealed cells equipped with windows of KBr and polyethylene and of the solid using cryostats cooled by liquid nitrogen. In spite of persistent attempts we never succeeded in obtaining a crystalline solid by annealing. Spectra were also obtained of the molecule trapped in argon and nitrogen matrices at ratios varying from 1:500 to 1:1000 using a closed cycle cryostat from Air Products. Before depositing on the cold window the sample/matrix gas was passed through a heatable quartz nozzle. Experiments were carried out at three different temperatures; 300, 475 and 910 K, but at the highest temperature pyrolysis was so severe that the experiment was abandoned. During the matrix experiments we found out that TCP adsorbs very strongly on metal surfaces. This led among other things to unwanted isotopic mixing when we recorded the matrix spectra of DTCP shortly after having worked with TCP.

The Raman spectra were recorded on a DILOR RTI 30 spectrometer (triple monochromator) using the 488 nm line of a CRL 52G argon ion laser for excitation. Spectra of the freshly distilled liquid were obtained, including semi-quantitative polarization measurements, and of the solid formed by shock freezing the vapour on a copper block cooled by liquid nitrogen. As was the case in the analogous IR experiments, we never obtained a crystalline solid by annealing.

Electron diffraction

Electron diffraction diagrams of TCP were recorded on Kodak Electron Image plates in the Balzers Eldigraph KDG-2 [23, 24] for two nozzle-to-plate distances. A doughnut shaped low-pressure nozzle [25] was used to minimize possible decomposition. The nozzle temperature was then 303 K which is about 30 degrees below that required by a conventional nozzle. The accelerating voltage was 42 kV and the electron wavelength $\lambda = 5.875$ pm as calibrated against diffraction patterns of gaseous benzene ($r_a = 139.75$ pm [26]). The estimated uncertainty in the s-scale is 0.1%.

The optical densities of the photographic plates were recorded as raster images on a modified Joyce-Loebl microdensitometer at the Department of Theoretical Astrophysics, University of Oslo. Six plates for the long (50 cm) and three plates for the short (25 cm) camera distances were used in the structure determination. Each of the short camera plates was densitometered twice.

ANALYSIS OF THE VIBRATIONAL DATA

The IR survey spectrum of TCP as a liquid at room temperature is reproduced in Fig. 2 while the corresponding Raman spectrum is given in Fig. 3. The observed wavenumbers are listed in Tables 1 and 2 for TCP and TCPD, respectively. The spectra of the amorphous solid are barely distinguishable from those of the liquid and have not been included in Table 1. Further, as all the bands appeared to be polarized in the Raman effect the polarization data have also been omitted from Table 1.

The matrix isolation spectra contain a large number of bands, some of which are obviously due to different trapping sites. For the sake of brevity, these bands have been omitted from Tables 1 and 2. Further, we only give the wavenumbers for the argon matrix experiments as the corresponding observations for the nitrogen matrix are almost identical. Some of the bands in the matrix isolation spectra show a systematic decrease in intensity with the annealing time and vanish from the spectra after ca. 20 h of annealing. These bands have been marked with asterisks in Tables 1 and 2.

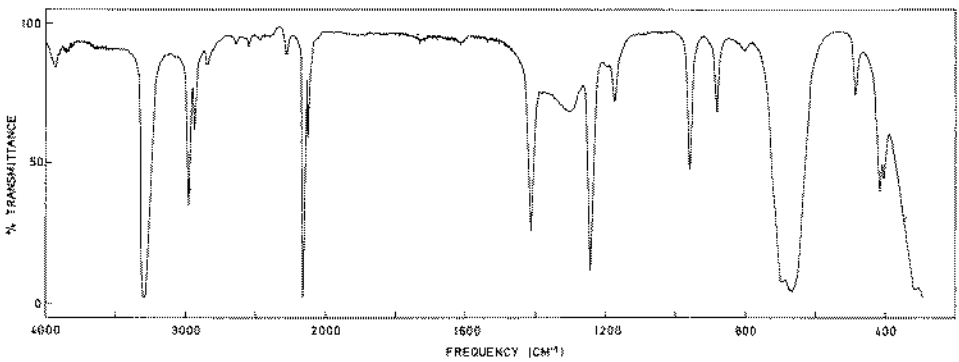

Fig. 2. Mid-IR spectrum of 3-thiocyanatopropyne as a liquid.

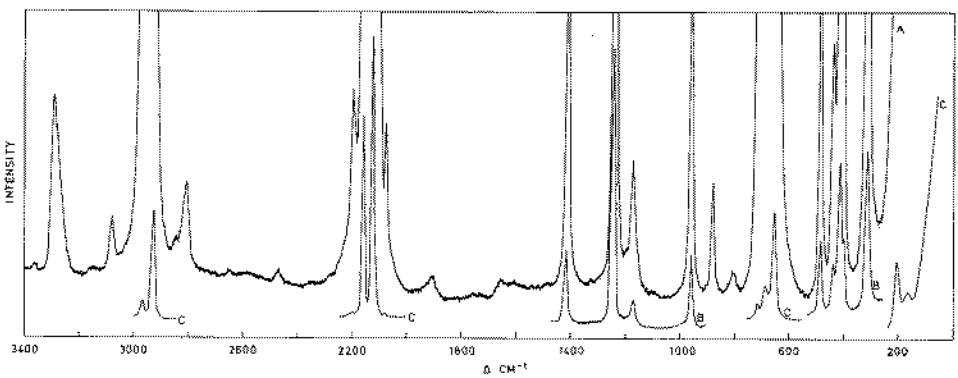

Fig. 3. Raman spectrum of 3-thiocyanatopropyne as a liquid.

TABLE 1

Infrared and Raman spectral data[a,b] for 3-thiocyanatopropyne (TCP)

IR		Raman	Interpretation	
Ar matrix	Liquid	Liquid	*anti*	*gauche*
3319 vs[b]	3290 vs,br	3293 m,br	$\nu_1\ a'$	ν_1
	~3075 vw	~3080 w		
	2974 m	2976 m	$\nu_{15}\ a''$	ν_2
	2934 w	2934 s	$\nu_2\ a'$	ν_3
	2914 vvw			
	2846 vw	2850 vw		
	~2810 vvw	2811 w		
	2280 vw	~2285 vvw		
	~2195 vvw	2196 m		
2166 m	2155 s	2158 vs	$\nu_3\ a'$	ν_4
2139 vw	2122 w	2126 vs	$\nu_4\ a'$	ν_5
		2077 m		
1429 m			$\nu_5\ a'$	
1413 m,*	1411 m	1412 s		ν_6
1342 w				
1330 w		~1330 vw		
1308 w,*				
1282 s	~1300 w,br			
1247 s,*				ν_7
	1240 s	1241 vs		
1235 s			$\nu_6\ a'$	
	~1200 vw	~1200 vvw		
1179 vw	1173 w	1173 m	$\nu_{16}\ a''$	ν_8
956 m	958 m	958 s	$\nu_7\ a'$	ν_9
933 w				
	~900 vvw	~900 vvw		
882 w,*				ν_{10}
	882 w	880 m		
874 vw			$\nu_{17}\ a''$	
	801 vw	805 vw		
729 s	720 m,sh	718 m	Acetylene	
702 s,*				ν_{11}
	693 s	~690 ms,br		
697 s			$\nu_8\ a'$	
684 mw				
666 vs			$\nu_9\ a'$	ν_{12}
653 s,*	~665 vs,br	656 s		ν_{13}
644 vs			$\nu_{18}\ a''$	ν_{14}
637 m			$\nu_{10}\ a'$	
486 w,*	485 w	489 m		ν_{15}
		440 m	$\nu_{11}\ a'$	
422 vw,*				ν_{16}
	415 m	416 s		
410 vw			$\nu_{19}\ a''$	
394 vw			$\nu_{12}\ a'$	
	401 m	402 m		
392 w				ν_{17}
317 s	315 s	314 s	$\nu_{20}\ a''$	ν_{18}
	200 w,br[c]	198 vs	$\nu_{13}\ a'$	ν_{19}
	165 w,br[c]	159 s		ν_{20}
	120 w,br[c]		$\nu_{14}\ a'$	

[a]Weak bands in the regions 4000–3400, 2700–2300 and 2000–1500 cm^{-1} have been omitted. [b] Abbreviations: s, strong; m, medium; w, weak; v, very; br, broad; *denote bands which disappear in the matrix spectra upon prolonged annealing. [c]From amorphous solid.

TABLE 2

Infrared spectral data[a,b] for 3-thiocyanatopropyne-1-[^{2}H] (DTCP)

IR	Interpretation		IR	Interpetation	
Ar matrix	*anti*	*gauche*	Ar matrix	*anti*	*gauche*
2607 vs	$\nu_2\ a'$	ν_3	881 vw,*		ν_{10}
2166 m	$\nu_3\ a'$	ν_4	699 w,*		ν_{11}
2005 m	$\nu_4\ a'$	ν_5	697 w	$\nu_8\ a'$	
1429 w	$\nu_5\ a'$		651 w,*		ν_{12}
1414 w,*		ν_6	636 w	$\nu_9\ a'$	
1246 m,*		ν_7	526 m	$\nu_{10}\ a'$	
1234 s	$\nu_6\ a'$		520 m,*		ν_{13}
1179 vw	$\nu_{16}\ a''$	ν_8	502 ms	$\nu_{18}\ a''$	ν_{14}
1054 vw			497 w		
1042 m,*			492 w		
1024 vw,*			488 vw,*		ν_{15}
1011 vw,*			477 vw		
1007 vw			405 vw	$\nu_{12}\ a''$	ν_{17}
944 vw	$\nu_7\ a'$	ν_9	306 s	$\nu_{20}\ a''$	ν_{18}
892 vw					

[a]Weak bands in the regions 4000–2700 and 2000–1500 cm^{-1} have been omitted. [b]Abbreviations: see footnote to Table 1.

Vibrational assignment

For the *anti* conformation of TCP with C_s symmetry the normal modes of vibration divide into $\Gamma_v = 15a' + 9a''$; the a' mode being polarized in the Raman effect. In the *gauche* conformation, C_1 symmetry, all bands should be polarized in the Raman effect.

The assignment of the fundamental modes of vibration for the two conformations of TCP relies to some extent upon the results from spectral studies on the 3-halopropynes [27, 28] and on 3-azidopropyne [29] and a close parallelism is found for the frequencies of vibration localized in the propynyl group.

As already noted, some of the bands observed in the spectra of the matrix isolated molecule show a systematic decrease in intensity with the annealing time and that they finally vanish completely from the spectra. This is an obvious indication of the presence of more than one conformation and allows an easy division of some of the matrix bands. As can be seen from Table 1, the corresponding bands in the liquid are unfortunately all overlapping and there is no way to associate either of the two groups of bands with a definite conformer. We have tentatively assigned the bands that remain in the matrix spectra after annealing to the *anti* conformer as the electron diffraction results indicate this conformation to be the more stable. We note, without including it as argument, that the band pair at 489/440 cm^{-1} corresponding to the C–C–S

bending modes give a clue to the conformational assignment. According to the normal coordinate calculations the C–C–S bending mode is definitely at higher wavenumbers in the *gauche* conformer than in the *anti*.

The vibrational interpretation is straightforward and needs only a few comments as most of the vibrations are characteristic group frequencies. The only complications arise from the 700–600 cm^{-1} region where four fundamentals for each conformer are expected, two C≡C–H bending modes and the two C–S stretching modes. In the spectra of the liquid only two bands are observed but, due to the smaller linewidths, seven bands can be seen in the spectra of the matrix isolated molecule. Upon deuteration the two strongest bands at 666 and 644 cm^{-1} disappear from the spectra and at the same time new bands appear around 520 and 500 cm^{-1}. Hence, the C≡C–H(D) bending modes are accounted for. Likewise, the band at 684 cm^{-1} is absent in the spectra of the deuterated compound, but this band must be due to a combination. The remaining four bands at 702, 697, 651 and 637 cm^{-1} show only minor isotopic shifts and according to the normal coordinate calculations (see later) the band pair at 702/697 cm^{-1} corresponds mainly to the $C_{(sp^3)}$–S stretching mode and consequently the 651/637 cm^{-1} band pair to the S–CN stretching mode. This assignment deviates from what has recently been suggested for thiocyanatoethane [7], where the $C_{(sp^3)}$–S and S–CN stretching modes have been assigned to 686 and 626 cm^{-1}, respectively.

The C–S torsional mode, expected below 100 cm^{-1}, has unfortunately not been observed in any of our spectra. This is the more regrettable as this mode is very important to the electron diffraction analysis.

Force field and calculation of vibrational quantities

A valence force field for TCP was constructed in part by transferring force constants from the 3-halopropynes and the alkylthiocyanates. These force fields were in turn developed from the existing vibrational data on the 3-halopropynes [27, 28], methylthiocyanate [1–4] and ethylthiocyanate [6–9]. Finally, the C–S torsional force constant was assumed to be 0.02 mdyn Å rad^{-2} corresponding to a frequency around 50 cm^{-1}. The transferred valence force constants were only slightly modified (Table 3) in order to obtain a good agreement with the observed wavenumbers as can be seen in Table 4. The established force field was used to calculate the root mean square amplitudes of vibration (l), perpendicular amplitude correction coefficients (K), and the centrifugal stretching (dR) of the interatomic distances as these quantities were needed in the analysis of the GED data as described below.

The structure determination based on the GED data employs geometrical models, and shrinkage corrections [30] have been implemented by the use of an r_α-model which specifies the TCP geometry in terms of r_α-type parameters. The corresponding set of geometrically consistent r_α interatomic distances were

TABLE 3

Suggested valence force constants for 3-thiocyanatopropyne (TCP)

Force constant	Value	Force constant	Value
Stretch (mdyn Å^{-1})		*Stretch/stretch* (mdyn Å^{-1})	
(≡)C–H	5.847	C–H/C–H	0.059
C≡C	16.130	C≡C/C–C	0.27
C–C	4.582	S–C(*sp*)/C≡N	0
C(sp^3)–S	2.996	(≡)C–H/C≡C	−0.070
S–C(*sp*)	4.404		
C≡N	16.424	*Stretch/bend* (mdyn rad^{-1})	
C–H	4.850		
		C–C/C–C–H	0.300
Bend (mdyn Å rad^{-2})		C(*sp*)–S/S–C–H	0.263
		C(sp^3)–S/C–C–S	0.799
HCH	0.423		
CCH	0.629	*Bend/bend* (mdyn Å rad^{-2})	
SCH	0.828		
CCS	1.148	SCH/SCH	0.111
CSC	0.700	SCH/CCH	0.030
C≡C–H (∥)[a]	0.241	SCH/CCH′	−0.020
C≡C–H (⊥)	0.226	CCH/CCH	−0.012
C≡C–C	0.294	CCH/HCH	0.020
S–C≡N	0.436	SCH/HCH	0.040
		HC≡C/C≡CC	0.099
Torsion (mdyn Å rad^{-2})		C≡CC/CCS	−0.035
		CCS/CSC (*gauche*)	−0.046
C–C–S–C	0.02	CCS/CSC (*anti*)	0.011
		CSC/SCN	−0.153

[a] ∥ and ⊥ signify parallel and perpendicular, respectively, to the plane defined by C≡C–C–S.

then converted to the geometrically inconsistent r_a counterparts required by the GED intensity expression by the relation $r_a = r_\alpha - D$, where $D = l^2/r - K - dR$ [30]. The magnitudes of the dR quantities, calculated as described elsewhere [31, 32], show that they should not be omitted in the computation of the distance conversion term, D.

Models which treat the large amplitude torsion about the C–S bond separately from the rest of the molecular dynamics [33] were also applied. These dynamic models, hereafter referred to as r'_α models, require framework vibrational quantities [30]. These l' and D' values are independent of the C–S torsional frequency (and force constant), and they were obtained by omitting contributions from the C–S torsional mode in the force-field calculations.

Calculated l, l', D and D' values for TCP at 303 K are given in Table 5. They were obtained using geometries consistent with those of the final structural results. Also, calculated l and l' values were used directly in the structure re-

TABLE 4

Observed and calculated fundamental frequencies of vibration (cm^{-1}) for 3-thiocyanatopropyne (TCP) and 3-thiocyanatopropyne-1-[^{2}H] (DTCP)

Conformer		TCP		DTCP		Approximate description
		Obs.	Calc.	Obs.	Calc	
Anti	*a'*	3319	3317	2607	2599	(≡)C–H(D) str.
		2934	2960	2934	2960	sym. CH_2 str.
		2166	2166	2166	2166	C≡N str.
		2139	2139	2005	1981	C≡C str.
		1429	1423	1429	1423	CH_2 scissor
		1235	1242	1234	1242	CH_2 wag
		956	958	944	948	C–C str.
		697	705	697	705	S–CN str.
		666	674	526	525	C≡C–H (D) bend
		637	651	636	660	C–S str.
		440	452	440	440	C–C–S bend
		394	397	402	395	C–C≡N bend
		198	199	198	192	C≡C–C bend
		120	123		120	C–S–C bend
	a''	2976	3000		3000	asym. CH_2 str.
		1179	1180	1179	1180	CH_2 twist
		874	875		874	CH_2 rock
		644	642	502	500	C≡C–H (D) bend
		410	423		422	S–C≡N bend
		317	314	306	304	C≡C–C bend
			58		57	C–S torsion
Gauche		3319	3317	2607	2599	(≡)C–H(D) str.
		2976	3001	2976	3001	asym. CH_2 str.
		2934	2960	2934	2959	sym CH_2 str.
		2166	2166	2166	2166	C≡N str.
		2139	2139	2005	1981	C≡C str.
		1413	1423	1414	1423	CH_2 scissor
		1247	1241	1246	1241	CH_2 wag
		1179	1180	1179	1180	CH_2 twist
		956	955	944	945	C–C str.
		882	881	881	881	CH_2 rock
		702	698	699	697	S–CN str.
		666	669	651	643	C–S str.
		653	639	520	527	C≡C–H (D) bend
		644	642	502	500	C≡C–H (D) bend
		486	473	488	460	C–C–S bend
		422	422		422	S–C≡N bend (bop)
		392	394		392	S–C≡N bend (bip)
		317	316	306	305	C≡C–C bend (bop)
		198	207		201	C≡C–C bend (bip)
		159	151		147	C–S–C bend
			52		51	C–S torsion

TABLE 5

Total (l, D) and framework (l', D') vibrational amplitude quantities[a] (pm) for the *gauche* (g) and *anti* (a) conformers of 3-thiocyanatopropyne (TCP) calculated from the force field of Table 3 (atomic numbering given in Fig. 1)

Type	$r_{(g)}/r_{(a)}$	$l_{(g)}/l'_{(g)}$	$l_{(a)}/l'_{(a)}$[b]	$D_{(g)}/D'_{(g)}$	$D_{(a)}/D'_{(a)}$
C_2–H_1	106.0	7.4		−3.8/−2.7	−4.3/−2.8
C_2≡C_3	120.8	3.6		−2.5/−1.2	−3.1/−1.3
C_3–C_4	144.7	4.9		−1.5/−0.4	−2.0/−0.4
C_4–S_5	184.0	5.4		−0.9/−0.4	−0.8/−0.1
S_5–C_6	169.0	4.4		−1.3/−0.2	−0.9/−0.4
C_6≡N_7	117.0	3.5		−1.5/−0.7	−1.2/−0.8
C_4–H_8	110.0	7.8		−2.9/−1.5	−3.4/−1.1
C_4–H_9	110.0	7.8		−2.8/−1.6	−3.4/−1.1
C_2···H_1	268	7.9		−4.7/−2.3	−5.8/−2.5
C_4···H_1	372	8.8		−4.7/−1.2	−6.3/−1.4
S_5···H_1	473	15.1		−2.2/−0.5	−2.9/−0.8
H_1···H_8	419	15.7		−5.3/−1.0	−7.8/−1.0
H_1···H_9	419	15.7		−5.9/−0.9	−7.8/−1.0
C_2···C_4	266	5.2		−2.8/−0.4	−4.0/−0.5
C_2···S_5	376	10.7		−0.9/−0.0	−1.1/−0.2
C_2···H_8	317	12.9		−3.7/−0.4	−5.7/−0.3
C_2···H_9	317	12.9		−4.3/−0.4	−5.7/−0.3
C_3···S_5	274	6.9		−4.7/−0.3	−0.3/−0.3
C_3···H_8	207	10.8		−2.9/−0.9	−4.2/−0.6
C_3···H_9	207	10.8		−3.5/−0.9	−4.2/−0.6
C_4···C_6	263	11.1		−0.6/−0.1	−1.3/ 0.3
C_4···N_7	356	13.0		−1.0/−0.1	−1.7/ 0.4
S_5···N_7	286	4.8		−2.0/−0.2	−1.4/−0.5
S_5···H_8	244	11.0		−2.8/−0.9	−2.7/−0.3
S_5···H_9	244	11.0		−2.2/−0.9	−2.7/−0.3
H_8···H_9	180	13.1		−3.9/−1.7	−4.7/−1.0
C_6···H_1	455/616	37.8/17.5	13.1/17.5	−1.0/−2.1	−1.3/−0.5
N_7···H_1	477/722	56.9/17.9	13.7/13.7	2.3/−3.2	−0.5/−0.2
C_2···C_6	373/513	31.8/12.2	10.4/10.4	0.3/−1.5	−0.2/ 0.0
C_2···N_7	413/617	46.3/11.5	11.8/11.8	2.2/−2.5	0.3/ 0.3
C_3···C_6	300/396	22.3/11.0	10.0/10.0	0.1/−1.2	0.0/ 0.1
C_3···N_7	365/497	30.1/12.6	12.0/12.0	0.1/−1.5	−0.1/ 0.2
C_6···H_8	362/280	12.5/12.5	21.8/16.9	−1.4/−0.7	−2.1/ 0.5
C_6···H_9	280/280	22.0/20.0	21.8/16.9	−1.2/−0.5	−1.9/ 0.9
N_7···H_8	462/354	13.9/13.9	27.2/19.9	0.1/ 0.8	−2.1/ 0.5
N_7···H_9	354/354	27.4/24.4	27.2/19.9	0.0/ 1.5	−1.9/ 0.9

[a] See text for definition of l and D.

[b] $l_{(g)} = l'_{(g)} = l_{(a)} = l'_{(a)}$ for torsional insensitive distances.

finements based on the GED intensities, either as fixed parameter estimates or to establish the relative magnitudes of l values in tied amplitude refinements.

CONFORMATIONAL AND STRUCTURAL ANALYSIS BASED ON THE GED DATA

The GED data of TCP were treated by standard data reduction methods [34] to yield the total electron-diffraction scattering intensities (actually $s^4 I_{tot}(s)$). The blackness correction applied on the measured densities (D) was $1.0+0.03D+0.09D^2+0.03D^3$. An automatic background subtraction routine, analogous to that described by Hedberg [35], was applied to the electron-diffraction scattering intensities in a modified form. The resulting intensity curves were scaled and averaged to yield one modified molecular intensity curve for each of the two camera distances (see Fig. 4). The corresponding experimental radial distribution curve (RD curve) is shown in Fig. 5.

The modification function [34] was $s/|f'_C(s)|^2$. The scattering amplitudes and phases [34] were calculated using the partial-wave method [36] based upon analytical Hartree–Fock potentials [37] for carbon, nitrogen and sulphur and the best electron density of bonded hydrogen [38] for the hydrogen atoms.

The structure analysis was carried out by the least-squares method based upon the intensity data shown in Fig. 4, using diagonal weight matrices. The standard deviations thus obtained (σ_{LS}) were augmented by a factor of two to

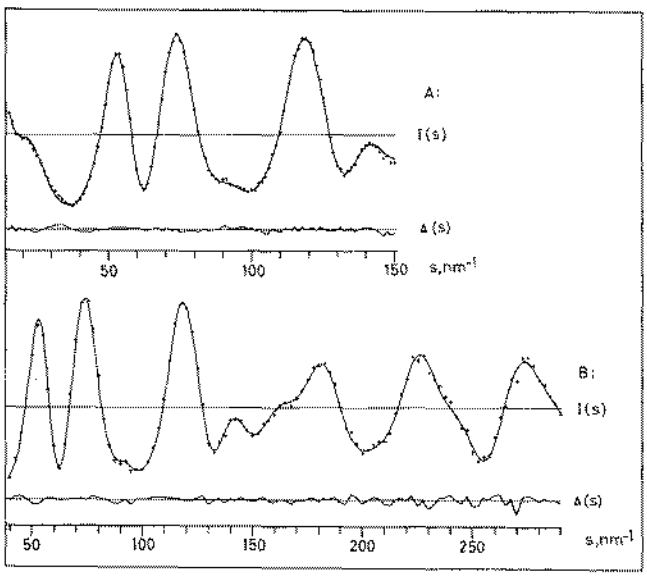

Fig. 4. Experimental (+) and final theoretical (full lines) molecular intensity curves ($I(s)$) for 3-thiocyanatopropyne (TCP) and the corresponding difference intensities ($\Delta(s)$, below).

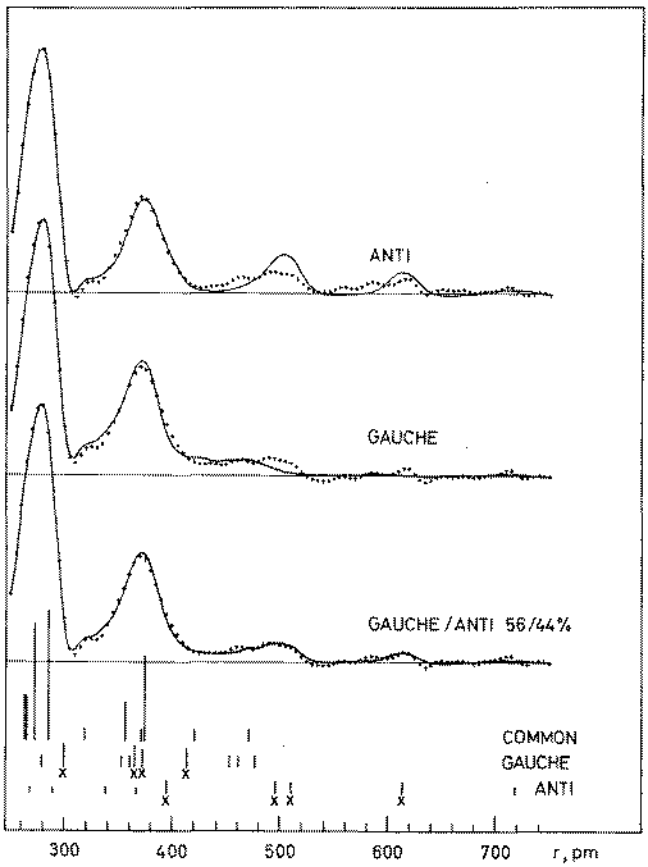

Fig. 5. Experimental (+) and final theoretical (full line) radial distribution curves (RD(r)) for 3-thiocyanatopropyne (TCP) and the corresponding difference curve (ΔRD(r)). The damping coefficient is 2.0×10^{-5} nm^2. The vertical bars show the interpretation of the RD curve in terms of three categories of interatomic distances: (a) common to both conformers; (b) those of the *gauche* conformer, and (c) those of the *anti* conformer.

account for correlation in the data. Data ranges and constants of the weighting scheme are specified in Table 6.

Interpretation of the RD-curve

The interpretation of the RD curve is illustrated by the line diagrams of Figs. 5 and 6 where the lines represent the twenty-one torsional independent distances (reduced from twenty-six in Table 5 due to coincidences), and ten torsion dependent distances. The positions and contributions of the latter type of distances determine the conformational properties of the molecule, the important distances being $C_3\cdots C_6$, $C_3\cdots N_7$, $C_2\cdots C_6$ and $C_2\cdots N_7$ (see Fig. 6). Introduc-

TABLE 6

Ranges and weighting of the electron-diffraction data[a]

Camera height (mm)	Data range			Constants of the weighting scheme[b]			
	s_{min}	s_{max}	Δs	*S1*	*S2*	*w1*	*w2*
497.59	15.0	150.0	1.25	50.0	100.0	0.0015	0.00055
247.64	40.0	290.0	2.50	50.0	160.0	0.0015	0.00008

[a]s values in nm, w values in nm^{-2}

[b]The two data sets were given equal weight; see ref. 34 for meaning of the symbols.

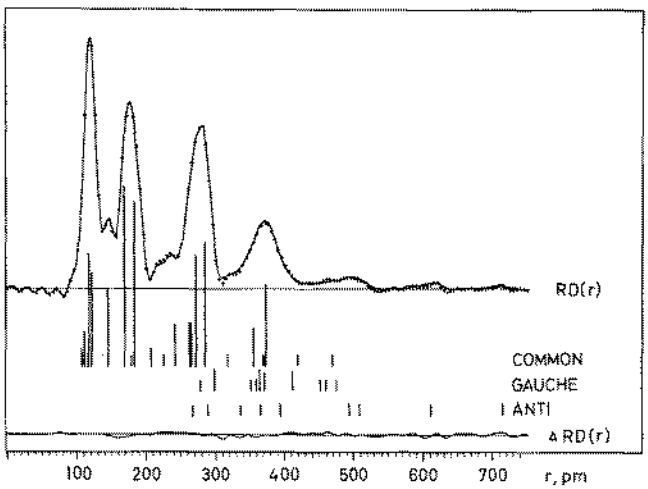

Fig. 6. The outer parts of experimental and calculated RD curves corresponding to one- and two-conformer interpretations of the GED data for 3-thiocyanatopropyne (TCP). The ×s in the line diagrams identify the important interatomic distances for the conformational analysis and they appear in the following order of increasing r values for both conformers: $C_3 \cdots C_6$, $C_3 \cdots N_7$, $C_2 \cdots C_6$ and $C_2 \cdots N_7$.

tory refinements omitting shrinkage corrections and constraining the amplitude parameters (l) to the calculated values (Table 5) revealed that there is a mixture of conformers at 303 K. The failure of a one-conformer interpretation of the data, in which *gauche* and *anti* forms were favoured over *skew* and *syn* forms, is demonstrated in Fig. 6. There are serious area-discrepancies between experimental and theoretical RD curves for *anti* and for *gauche* and the corresponding agreement factors based on the intensities are 9.5% and 8.4%, respectively. A good fit (R=6.7%) was obtained, however, for a *gauche–anti* ratio of 56–44% as also demonstrated in Fig. 6. Appropriate models were used in the background correction procedure for each of these interpretations.

Model specifications

Perspective views of the *gauche* and *anti* forms of TCP showing the numbering of the atoms are presented in Fig. 1. The geometry of one conformer of TCP was ultimately described by the twelve parameters listed in Table 7 constraining those concerning the locations of the hydrogen atoms to values as specified in the table. The β-parameter, which is the in-plane (C_3–C_4–S) tilt of the CH_2 group from the bisector of the C_3–C_4–S angle, was fixed at 1° as suggested by results of introductory refinements. Linearity was assumed at C_2, C_3 and C_6, as various fixed magnitudes of bending parameters did not give any improved fit to the data or significant shifts in the values for the other important structural parameters. Bending of S–C≡N was also tested at the final stage of the analysis, but the above conclusion was maintained.

Introduction of two torsional angles, φ_g and φ_a, and a composition parameter, α ($\alpha = \alpha_g$; $\alpha_a = 1.00 - \alpha_g$), provided the required possibility of a two-conformer interpretation of the GED data then assuming that any two conformers only differ geometrically in the torsional angle. The validity of this assumption

TABLE 7

Structural parameters (pm, degrees) for 3-thiocyanatopropyne (TCP)[a]

Distance	Model			Angle	Model	
	r_α	r'^{c}_α			r_α	r'_α
≡C–H	102.0(–)	103.3(–)	[102.0]	C–S–C	97.6(9)	97.4(10)
C–H	106.9(–)	108.7(–)	[106.9]	C–C–S	113.7(6)	112.7(6)
C≡N	115.5(3)	116.0(3)	[115.4]	H–C–H	109.5(–)	109.5(–)
C≡C	117.7(4)	119.4(5)	[117.8]	β	1.0(–)	1.0(–)[e]
C–C	142.8(4)	144.0(4)	[142.7]	ϕ_g	57.(8)	53(5)
S–C_{sp}	167.8(2)	168.6(2)	[167.8]	ϕ_a	171(12)	180(–)
S–C_{sp^3}	182.7(2)	183.3(2)	[182.6]	δ_g	–	13(4)
				δ_a	–	20(7)[f]
Composition (%)				*Dependent angles*[g]		
α_g	59(6)	55(6)		C–C–H	107.9(2)	108.1(2)
α_a	41(6)	45(6)		S–C–H	108.9(2)	109.1(2)
Agreement factor (%)[d]						
R	5.14	5.03				

[a]Values in parentheses are estimated standard deviations (σ) accounting for data correlation and for the distance parameter uncertainties in the s-scale, $\sigma = [(2\sigma_{LS})^2 + (0.001r)^2]^{\frac{1}{2}}$; (–) signifies that the parameter was not refined. [b]r_α Values ($r_\alpha = r_a + D$). [c]r_α Values ($r_\alpha = r_a + D'$); corresponding r_α-type distances in square brackets. [d]$R = 100\ [\sum w_i \Delta_i^2 / \sum w_i I_i^2(\mathrm{obs})]^{\frac{1}{2}}$; $\Delta_i = I_i(\mathrm{obs}) - I_i(\mathrm{calc})$. [e]$\beta$ is the in-plane (C_3C_4S) tilt of the CH_2 group from the bisector of the C_3C_4S angle. [f]This value was obtained in a previous refinement with the l_1–l_8 amplitude parameters fixed at values consistent with those given in Table 8. [g]Standard deviations do not include the uncertainty in β.

TABLE 8

Interatomic distances (r_a) and vibrational amplitudes (l) (pm) in 3-thiocyanatopropyne (TCP) corresponding to the results for the r_α-model of Table 7[a]

Type[b]	r_a	l[c]
	gauche/anti	*gauche/anti*
C_2–H_1	106.0/106.1 fixed	7.5(4) l_1
C_4–H_8	110.2/109.8 fixed	7.8(4) tied (l_1)
C_4–H_9	110.3/109.8 fixed	7.8(4) tied (l_1)
C_6≡N_7	116.7/116.8(4)	3.6(4) tied (l_1)
C_2≡C_3	120.6/120.7(5)	3.6(4) tied (l_1)
C_3–C_4	144.4/144.4(4)	5.0(4) l_2
S_5–C_6	168.8/169.0(3)	5.0(4) l_3
C_4–S_5	183.7/183.4(3)	5.4(4) l_4
C_3··H_1	225.0/225.2(5)	7.9 fixed
C_3··H_8	207.8/207.6(5)	12.2(22) l_5
C_3··H_9	207.8/207.6(5)	12.2(22) tied (l_5)
S_5··H_8	241.4/240.7(4)	12.4(22) tied (l_5)
S_5··H_9	241.4/240.7(4)	12.4(22) tied (l_5)
C_4··C_6	264.7/264.3(19)	10.9(9) l_6
C_2··C_4	263.8/264.0(6)	5.0(9) tied (l_6)
S_5··C_3	273.6/273.6(9)	8.2(5) l_7
S_5··N_7	284.7/285.0(4)	6.0(5) tied (l_7)
C_4··N_7	375.9/357.5(26)	15.7(11) l_8
S_5··C_2	374.6/375.8(13)	13.4(11) tied (l_8)
C_3··C_6	296(4)/397(1)	11.0/10.0 fixed
C_3··N_7	360(6)/498(2)	12.6/12.0 fixed
C_2··C_6	366(7)/512(1)	12.2/10.4 fixed
C_2··N_7	403(11)/616(2)	11.5/11.8 fixed

[a]See footnote a to Table 7. [b]See Fig. 1 for numbering of the atoms. The other interatomic distances (see Table 5) were included in the refinement, but are not listed here. [c]l_1–l_8 identify the independent l-values or l-value groups refined; cf. Table 5 for l-value differences within each group, and for fixed parameter values.

was in particular tested for the C_3–C_4–S angle in view of subsequent results for the $l(C_3\cdots S)$ parameter and by results of ab initio MO calculations for the azide analogue, HC≡7C–CH_2N_3 [29]. However, this relaxation of the model did not solve the l-value problem nor give an improved fit to the data. In fact, the difference parameter for the C_3C_4S angles in the two conformers refined to zero.

Anti conformations with φ_a values of 161(8)–168(8)° were obtained when shrinkage corrections were omitted. Also, the r_α model gave slight deviations from C_s symmetry (cf. Table 7). This could suggest a double minimum about

TABLE 9

Standard deviations (σ_{LS}) and correlation matrix (100 ρ_{ij}) for the parameters of the final r_α refinement

Type[a]	σ_{LS}	ρ_{ij}								
C=N	0.15	100								
C≡C	0.21	−86	100							
C–C	0.18	17	−9	100						
S–C_6	0.11	−34	27	27	100					
S–C_4	0.12	−1	2	54	33	100				
C–S–C	0.43	46	−51	−24	−22	−20	100			
C–C–S	0.32	−35	27	−51	−31	−44	−24	100		
φ_g	4.1	−2	8	37	25	25	−52	−41	100	
δ_g	6.1	54	−56	−8	−17	−9	65	−3	−39	100
l_1	0.17	73	−75	27	−25	8	32	−28	2	51
l_2	0.22	−21	9	−1	40	12	−4	−5	2	−11
l_3	0.20	−5	0	−45	3	−55	9	24	−10	12
l_4	0.20	−11	7	−26	32	−28	−2	7	3	6
l_5	1.1	−12	14	−4	13	1	−35	1	24	−20
l_6	0.43	22	−16	7	9	7	30	−60	14	22
l_7	0.23	−30	26	−15	−26	−10	11	50	−55	22
l_8	0.64	5	−2	5	3	3	8	−43	32	−39
α_g	3.1	0	4	−3	−5	−12	−1	10	18	12
Sc(l)	0.18	38	−34	16	−21	3	12	−13	8	36
Sc(s)	0.24	30	−27	11	−20	2	12	−7	0	34

$\varphi = 180°$, but also that the applied shrinkage correction, which was based on a guessed C–S torsional frequency, was inappropriate. In the dynamic r'_α models used in the present investigation both the *anti* and the *gauche* form of TCP are specified using the respective r.m.s. torsional angle amplitudes for harmonic torsional potentials (δ_a and δ_g). These parameters give information about the corresponding torsional force constants by the relation $F_\tau = RT\delta^{-2}$ [33]. Each conformer was represented by nine pseudo conformers ($\varphi_i = \varphi \pm \Delta\varphi_i$; $\Delta\varphi_i = 0$, $\frac{1}{2}\delta$, δ, $\frac{3}{2}\delta$ and 2δ). They are weighted according to Gaussian potential curves and have framework vibrational properties (l' and D' in Table 5). The *anti* conformer has C_s symmetry and the number of pseudo conformers is reduced to five. The large-amplitude treatment of the *gauche* form is still based on a harmonic torsional potential which is certainly not correct, but nevertheless represents a better model than the harmonic r_α model based on small amplitude vibrations.

It should be noted that, unlike the l and l' values, the r_α to r_a conversion terms (D) depend on the perpendicular amplitude coefficients (K) yielding $D(g) \neq D'(g) \neq D(a) \neq D'(a)$ for all interatomic interactions including those associated with bond distances (cf. Table 5). In order to make the shrinkage corrections straightforward we have chosen to include the full set of r_a dis-

TABLE 9

Type[a]	σ_{LS}	ρ_{ij}									
C≡N											
C≡C											
C–C											
S–C_6											
S–C_4											
C–S–C											
C–C–S											
φ_g											
δ_g											
l_1	100										
l_2	−25	100									
l_3	0	0	100								
l_4	0	12	79	100							
l_5	−15	3	18	29	100						
l_6	22	−4	14	24	38	100					
l_7	−5	−14	10	4	2	−2	100				
l_8	3	0	−2	−1	−5	19	−33	100			
α_g	4	−6	3	0	−10	−10	4	19	100		
Sc(l)	63	−36	21	20	−13	23	16	3	11	100	
Sc(s)	64	−18	22	22	−10	21	24	0	10	60	100

[a]See Tables 7 and 8. Distances and l values in pm, angles in degrees, α in %. Sc(l) and Sc(s) are the scale factors for the long and short camera distance data sets.

tances for both conformers (Table 8). As a matter of convenience all geometrical assumptions apply to the r_α-type or the r'_α-type parameters rather than to the r_a distances. The geometrical parameters of the r_α and r'_α models (Table 7) have different physical meaning, and the r_α counterparts to the r'_α-type distance parameters, calculated from pertinent r_a and D values (Tables 8 and 5, respectively), have been included in Table 7.

RESULTS AND DISCUSSION

The present GED study of TCP is the first of its kind on organic thiocyanates and as such the molecule is particularly ill-chosen as the analysis is hampered by severe distance overlaps. It should be noted, however, that at the outset the GED study was mainly intended to clarify the conformational properties of gaseous TCP. As it turned out an elaborate structural analysis was needed in order to get reliable information about the conformational equilibrium.

The results of the final refinements of the r_α and r'_α models are given in Table 7. Eight independent l values or l value groups, as specified in Table 8, were

TABLE 10

Comparison of some of the geometrical parameters (pm, degrees) of 3-thiocyanatopropyne (TCP) with related molecules

Molecule	Method	$r_{C\equiv C}$	r_{C-C}	$r_{C\equiv N}$	$r_{S-C(\equiv)}$	r_{S-C}	∠CCS	∠CSC	Ref.
HC≡C–CH_2–S–C≡N	ED, r_a	120.7(5)	144.4(4)	116.8(4)	168.9(3)	183.6(3)	112.7(6)	97.4(10)	This work
HC≡C–CH_2–N=N≡N	ED, r_a	121.6(7)	148.1(13)				[114.5(15)]		29
HC≡C–CH_3	MW, r_s	120.6	145.9						41
	MW, r_0	120.7(5)	145.8(5)						42
HC≡C–CH_2CH_2–C≡CH	ED, r_a	122.0(5)	145.9(1)				[110.7(3)]		43
N≡C–CH_2CH_2–C≡N	ED, r_a		146.5(2)	116.1(2)			[110.4(5)]		44
CH_3–C≡N	MW, r_s		145.8(3)	115.7(3)					41
	ED/MW, r_g		146.8(2)	115.9(4)					45
CH_3–S–C≡N	MW, r_s			117.0(2)	168.4(3)	182.4(2)		99.03(8)	11
N≡C–S–C≡N	MW, r_s			115.7(2)	170.1(2)			98.37(17)	46
CH_3–S–CH_3	ED, r_g					180.7(2)		99.05(4)	47
HC≡C–S–CH_3	MW	120.5(7)			168.5(5)	181.3(2)		99.92(17)	48
	ED	121.5(3)			168.2(3)	181.4(3)		100.0(5)	48
R–CH_2–S–C≡N	XR			114.0(5)	167.7(5)	182.1(5)	113.6(3)	100.0(3)	13–17

included in these refinements which both gave least-squares agreement factors of about 5.1% as compared to about 6.2% when all amplitudes had values obtained from the force field calculations (Table 5). Refinements of l values associated with the torsion-dependent distances were not successful, but the δ-parameters of the r'_α model could be determined in a partly iterative way (see footnote e in Table 7).

It is believed that the r'_α model provides the best and most flexible treatment of the vibrational situation of the molecule. Hence it should also yield the most reliable determination of the structural and compositional parameters and our final results are those obtained by refinements of this model (cf. Tables 7–9). The corresponding difference intensities and the difference RD curve are shown in Figs. 4 and 5, respectively. They demonstrate together with the R factor that the fit to the experimental data is good.

The vibrational parameter values obtained for the bonded interactions (Table 8) are close to their calculated counterparts (Table 5), with the exception of that for the S–C≡ interaction which is 5.0(4) pm as compared to the calculated value of 4.4(4) pm. Attempts to tie this parameter to l_2 (cf. Table 8) caused convergence problems. The l values obtained for the non-bonded interactions were also too large, and these discrepancies were not removed by relaxation of various model constraints as discussed previously. It should be noted that a concurrent GED study based on data obtained both with a conventional and a low-pressure nozzle showed that the latter experimental set-up gave too high values for non-bonded amplitude parameters including the torsional-angle amplitudes, δ [39].

The C_4–S_5 torsional force constants may be calculated from the obtained δ values $F_\tau = RT\delta^{-2}$ [33]: $F_\tau(gauche) = 0.08(5)$ and $F_\tau(anti) = 0.03(2)$ mdyn Å rad^{-2} suggesting torsional frequencies of 104 and 71 cm^{-1} for the *gauche* and *anti* conformer, respectively. However, these evaluations are rather uncertain due to the large standard deviations and difficulties in determining the δ parameters from the GED data. The interplay between GED and spectrosopy is, in the present case, further obscured by the possibility mentioned of a systematic experimental error which most likely results in too large δ values. This would, however, remove the estimated torsional force constant even more from those used in the force field calculations ($F_\tau(gauche) = F_\tau(anti) = 0.02$ mdyn Å rad^{-2}) corresponding to torsional frequencies around 50 cm^{-1}.

Gauche was found to be marginally the dominating conformer of TCP at 303 K through all stages of refinements (α_g: 52(7)%–61(6)%). The energetically favoured form may be found by relating the determined *anti*⇌*gauche* equilibrium constant, $K = \alpha_g/\alpha_a = 1.22$, to the thermodynamic functions $\Delta H^0 = H^0_g - H^0_a$ and $\Delta S^0 = S^0_g - S^0_a$. The statistical weight of two, accounting for the existence of two identical *gauche* forms, should be included in the entropy term which may be written $\Delta S^0 = R\ln 2 + \Delta S^0_c$, where ΔS^0_c is the difference in confor-

tional entropies. In the present investigation we have no determination of ΔS_c^0 which would require variable temperature GED data or spectroscopic data with reliable assignments of all normal modes (in particular the low-frequency modes) for both conformers. However, ΔS_c^0 is often assumed to be negligible giving for TCP, $\Delta H^0 = -R \times T \times \ln K + R \times T \times \ln 2 + T \times \Delta S_c^0 \approx 1.24$ kJ mol^{-1} indicating that *anti* is most likely the low energy conformer. It should be noted, however, that the energy difference is small and that the conclusion could be reversed if *anti* were clearly the high entropy form as $\Delta H^0 < 0$ for $\Delta S_c^0 < -4.1$ J K^{-1} mol^{-1}.

The structural parameters of TCP are compared with literature vapour phase data for related molecules in Table 10. Although a comparison of structural parameters determined by microwave spectroscopy/electron diffraction and by X-ray diffraction is not entirely justifiable, we have also included the mean values of the structural parameters from X-ray studies of molecules containing the CH_2–SCN fragment [12–14, 16, 17]. As can be seen, the structural parameters comply well, thus justifying the assumptions in the applied model (identical structural parameters for the two conformers and linear HCCC and SCN chains) and adding credibility to the found conformational composition.

Concerning the preferred conformation around the C–S(CN) bond, it must be noted that X-ray studies of molecules containing the C–CH_2–SCN fragment [12, 13, 16, 17] show the conformation always to be *gauche*. As mentioned earlier, the preferred conformation of ethylthiocyanate is also *gauche* in all phases [6, 7, 19]. The fact that *anti* probably is the more stable form in TCP can be explained by a dipolar repulsion, which is easily visualised by performing a vectorial addition of the dipole moments of propyne [40] and methylthiocyanate [11].

ACKNOWLEDGEMENT

We are grateful to Mr. Hans V. Volden and Mrs. Snefrid Gundersen for recording the electron diffraction data and to Mr. H. Priebe for assistance in the synthesis of TCP.

REFERENCES

1 N. S. Ham and J. B. Willis, Spectrochim. Acta, 16 (1960) 279.
2 F. A. Miller and W. B. White, Z. Elektrochem., 64 (1960) 701.
3 A. G. Moritz, Spectrochim. Acta, 22 (1966) 1021.
4 G. A. Crowder, J. Mol. Spectrosc., 23 (1967) 108.
5 R. Vogel-Hogler, Acta Phys. Austriaca, 1 (1948) 311.
6 G. O. Braathen and A. Gatial, Spectrochim. Acta, Part A42 (1986) 615.
7 J. R. Durig, J. F. Sullivan and H. L. Heusel, J. Phys. Chem., 88 (1984) 374.
8 O. H. Ellestad and T. Torgrimsen, J. Mol. Struct., 12 (1972) 79.
9 R. P. Hirschmann, R. N. Kniseley and V. A. Fassel, Spectrochim. Acta, 20 (1964) 809.

10 C. E. Sjøgren, Acta Chem. Scand., Ser. A, 38 (1984) 657.
11 H. Dreizler, H. D. Rudolf and H. Schleser, Z. Naturforsch., Teil A, 25 (1970) 1643.
12 D. Jinbi, Z. Jiping, W. Yexin and W. Guanli, J. Struct. Chem. (Jiegou Huaxue), 2 (1983) 101.
13 K. Maartmann-Moe, K. A. Sanderud and J. Songstad, Acta Chem. Scand., Ser. A, 38 (1984) 187.
14 R. Bringeland and O. Foss, Acta Chem. Scand., 12 (1958) 79.
15 J. H. Konnert and D. Britton, Acta Crystallogr., Sect. B, 27 (1971) 781.
16 B. Tashkhodzhaev, S. Akhmedova and N. K. Rozhkova, Zh. Strukt. Khim., 21(2) (1980) 137.
17 J. Kaiser, R. Richter, J. Seiler, K. Schulze and M. Muhlstadt, Acta Crystallogr., Sect. B, 33 (1977) 879.
18 A. Bjørseth and K. M. Marstokk, J. Mol. Struct., 11 (1972) 15.
19 G. Gundersen and T. Midtgaard, unpublished results.
20 J. Medina, V. De Santis and N. Barroeta, Phosphorus Sulfur, 1 (1976) 281.
21 R.J. Maxwell, P. E. Pfeffer and L.S. Silbert, J. Org. Chem., 42 (1977) 1520.
22 L. Brandsma and H.D. Verkruijsse, Synthesis of Acetylenes, Allenes and Cumulenes, Elsevier, Amsterdam, 1981.
23 W. Zeil, J. Haase and L. Wegmann, Z. Instrumentenkd., 74 (1966) 84.
24 O. Bastiansen, R. Graber and L. Wegmann, Balzers' High Vacuum Rep., 25 (1969) 1.
25 R. Seip and H. V. Volden, The Norwegian Electron Diffraction Group, Annu. Rep., 1980, p. 7.
26 K. Tamagawa, T. Iijima and M. Kimura, J. Mol. Struct., 30 (1976) 243, and references cited therein.
27 J. C. Evans and R. A. Nyquist, Spectrochim. Acta, 19 (1963) 1153.
28 R. A. Nyquist, T. L. Reder, F. F. Stec and G. J. Kallas, Spectrochim. Acta, Part A, 27 (1971) 897.
29 J. Almlöf, G. O. Braathen, P. Klaeboe, C. J. Nielsen, H. Priebe and S. H. Schei, J. Mol. Struct., 160 (1987) 1.
30 K. Kuchitsu and S. J. Cyvin, in S. J. Cyvin (Ed.), Molecular Structures and Vibrations, Elsevier, Amsterdam, 1972, Chap. 12.
31 M. Iwasaki and K. Hedberg, J. Chem. Phys., 36 (1962) 2961.
32 R. L. Hildebrandt and J. D. Wieser, J. Chem. Phys., 42 (1966) 4648.
33 K. Hagen and K. Hedberg, J. Am. Chem. Soc., 95 (1973) 1003.
34 B. Andersen, H. M. Seip, T. G. Strand and R. Stølevik, Acta Chem. Scand., 23 (1969) 3224.
35 L. Hedberg, Abstr. Fifth Austin Symp. on Gas Phase Mol. Struct., Austin, TX, March 1974, p. 37.
36 A. C. Yates, Comput. Phys. Commun., 2 (1971) 175.
37 T. G. Strand and R. A. Bonham, J. Chem. Phys., 40 (1964) 1681.
38 R. F. Stewart, E. R. Davidson and W. T. Simpson, J. Chem. Phys., 42 (1966) 3175.
39 G. Gundersen, F. Karlsson, Z. Smith and H. G. Thomassen, Acta Chem. Scand., Ser. A, 40 (1986) 522.
40 R. L. Shoemaker and W. H. Flygare, J. Am. Chem. Soc., 91 (1969) 5417.
41 C. C. Costain, J. Chem. Phys., 29 (1958) 864.
42 L. F. Thomas, E. I. Sherrard and J. Sheridan, Trans. Faraday Soc., 51 (1955) 619.
43 M. Traetteberg, P. Bakken, S. J. Cyvin, B. N. Cyvin and H. Hopf, J. Mol. Struct., 51 (1979) 77.
44 L. Fernholt and K. Kveseth, Acta Chem. Sand., Ser. A, 33 (1979) 335.
45 K. Karakid, T. Fukuyama and K. Kuchitsu, Bull. Chem. Soc. Jpn., 47 (1974) 299.
46 L. Pierce, R. Nelson and C. Thomas, J. Chem. Phys., 43 (1965) 3423.
47 T. Iijima, S. Tsuchiya and M. Kimura, Bull. Chem. Soc. Jpn., 50 (1977) 2564.
48 (a) D. den Engelsen, J. Mol. Spectrosc., 30 (1969) 474, and references cited therein.
(b) B. P. van Eijck, to be published.